Journal of the Iranian Chemical Society (2021) 18:1279–1288
https://doi.org/10.1007/s13738-020-02112-9

ORIGINAL PAPER

Acceptor substituent effect on triphenylamine-based organic dye sensitizers for DSSCs: quantum chemical study

Raman Govindarasu[1] · Muthugoundar Karuppugoundar Subramanian[1] · Ammasi Arunkumar[2] · Shajahan Shanavas[2] · Ponnusamy Munusamy Anbarasan[2] · Tansir Ahamad[3] · Saad M. Alshehri[3]

Received: 1 September 2020 / Accepted: 27 October 2020 / Published online: 2 January 2021

Abstract

In this work, a series of triphenylamine (TPA)- based dye molecules (A1–A5) for dye-sensitized solar cells (DSSCs) application has been designed and screened. The electron donor contains TPA, thieno[3,2-b]thiophene, as the π-bridge, cyanoacrylic acid as electron acceptor based on donor–π-spacer–acceptor (D-π-A) as reference dye (3a). In order to enhance the tuning, effect of acceptor moieties was investigated at 3a dye. The electron acceptor effect of the substituent on the absorption spectra and photovoltaic (PV) properties has been investigated by the combination of density functional theory (DFT) and time-dependent DFT (TD-DFT) method approaches. Different exchange-correlation (XC) functionals were initially evaluated in order to establish a proper methodology for calculating the excited state energy of the 3a dye. Consequently, TD-ωB97XD method and 6-31G(d) basis set have used the comparison of experimental value. From the calculated results, it was concluded that the A4 (PO_3H_2) and A5 (SO_2H) dyes are strongly grouped for more red-shift and electrons injected into semiconductor the conduction band edge of TiO_2 was successful. It is expected that our research will pave a new method to design efficient organic D-π-A dye sensitizers in DSSCs.

Keywords Organic dye · DFT and TD-DFT · Exchange-correlational functional · Electronic and absorption spectra

Introduction

Organic dye-sensitized solar cells (DSSCs) as a promising applicant for a new generation of photovoltaic (PV) devices, the so-called Gratzel cell first developed in 1991, convert solar energy into electricity [1]. A characteristic DSSCs contain key components: a photosensitized dye-coated photoanode (conduction band edge (CBE) of the semiconductor TiO_2), redox shuttle, and a counter electrode [2]. As one of the crucial parts of DSSCs, the dye sensitizer affects the power conversion efficiency (PCE) owing to their grave function in electron injection and light-harvesting. Upon light irradiation, photoinduced electron injection ensues from the excited dye into the CBE of the TiO_2 surface. In DSSCs, sensitizers can be divided into two categories: (i) metal complex and (ii) metal-free organic dye, and it has been made to improve the PCE of DSSCs. Recently, PCE was reaching up to 24.2%, showed by a scientific research statement, but the conventional electricity production process is still non-competitive [3]. Most traditional organic dye sensitizers contain the structure of donor-π-bridge-acceptor (D-π-A). Commonly, organic sensitizers used for efficient solar cells are required to possess wide and extreme absorption in the visible spectral region [4–7]. Other major advantages of the organic dyes are ease of structural modification, low cost of device manufacture and photoelectrochemical properties compared to metal-based dyes [8, 9]. Recently, merocyanine [10], cyanine [11], hemicyanine [12], triphenylamine [13–16], dialkylaniline [17],

Supplementary Information The online version contains supplementary material available at (https://doi.org/10.1007/s13738-020-02112-9).

✉ Muthugoundar Karuppugoundar Subramanian
profdrmks@gmail.com

✉ Ponnusamy Munusamy Anbarasan
profpmanbarasan@gmail.com

[1] PG and Research Department of Physics, Thiruvalluvar Goverment Arts College, Rasipuram, Namakkal 637401, India

[2] Department of Physics, Periyar University, Salem 636 011, India

[3] Department of Chemistry, College of Science, King Saud University, P.O. Box 2455, Riyadh 11451, Saudi Arabia

phenothiazine [18], tetrahydroquinoline [19], coumarins [20–23], indoline [24–27], and carbazole [28] dyes have been tested and applied in DSSCs successfully. For example, N, N′-dialkylaniline based on (NDI 6) dye sensitizer used in DSSCs were revealed a PCE is 19.24%, reported by kar groups [29].

Highly efficient organic dye sensitizers for DSSCs must have the following properties [30]: First, the dye absorbs most of the sunlight, a broad absorption range that covers both the visible and near-infrared regions. Second, intramolecular charge transfer (ICT) from electronic donor to acceptor is one of the characteristics of organic dyes in DSSCs [31]. Third, suitable energy levels of the highest occupied molecular orbitals (HOMOs) of the dyes must be below the redox potential of the electrolyte (I^-/I_3^-). Besides, the lowest unoccupied molecular orbitals (LUMOs) of the dyes must be above the CBE of TiO_2 metal oxide surface. Accordingly, all dye molecules in the excited state of electrons can be efficiently injected into the TiO_2 surface. Particularly, D-π-A structure in the acceptor part is directly connected to the semiconductor surface, which favors efficient charge transfer (CT) from excited dye to the CBE of semiconductor, and thus improving regeneration of dyes by the redox couple [32].

In 2017, S.M. Fernandes [33] synthesized a D-π-A-based 3a is a simple structure of the organic chromophore with the TPA group as a donor, thieno[3,2-b]thiophene as a spacer and cyanoacetic acid as acceptor. As per the 3a, device exhibits a PCE is 3.68%, photocurrent (9.52 mA cm^{-2}) and photovoltage (0.600 V) measured under AM 1.5G irradiation. Furthermore, PCE of the DSSCs is predominantly determined by the short-circuit current density (J_{SC}), open-circuit photovoltage (V_{OC}) and the fill factor (FF). The improvement J_{SC} and V_{OC} will significantly enhance the PCE. Additionally, the acceptor group of the dye plays a key role in the semiconductor surface and improving the efficiency of the solar cell performance.

Here, CSSH, CONHOH, OH, PO_3H_2 and SO_2H dyes were used as the substituted acceptor groups [34]. The substituent groups of the acceptor were denoted as (A1–A5). Scheme 1 displays the electron-acceptor-based D-π-A sensitizers was under investigation, to affect the light-harvesting ability and conversion efficiency. In this work, a detailed study on photosensitizing properties of some metal-free organic dye derivatives has been studied using density functional theory (DFT) and time-dependent DFT (TD-DFT) methods approach. The calculated results represented the future experimental studies to plan and fast screen new organic efficient sensitizers for DSSCs.

Computational methodology

Theoretical background

The sunlight-to-electricity conversion efficiency (η) is mainly determined by the J_{SC},V_{OC}, FF and the intensity of incident light (P_{INC}), it can be stated as follows [35]:

$$\eta = \frac{J_{SC} V_{OC} \mathrm{FF}}{P_{INC}} \tag{1}$$

In DSSCs, J_{SC} is connected to the communication among TiO_2 and the dye sensitizers, along with the absorption coefficient of the designed dye molecules. It can be defined by the following equation [36]:

$$J_{SC} = \int \mathrm{LHE}(\lambda) \Phi_{\mathrm{inject}} \eta_{\mathrm{collect}} \, \mathrm{d}\lambda \tag{2}$$

In which, LHE is the light-harvesting efficiencies at a certain wavelength, Φ_{inject} denotes the quantum yield of electron injection and η_{collect} is the efficiency for charge collection efficiency. For DSSCs, the electrodes are similar but only different in dye sensitizers. Hence, it is judicious to adopt

Scheme 1 Sketching of molecular structure for electron acceptor

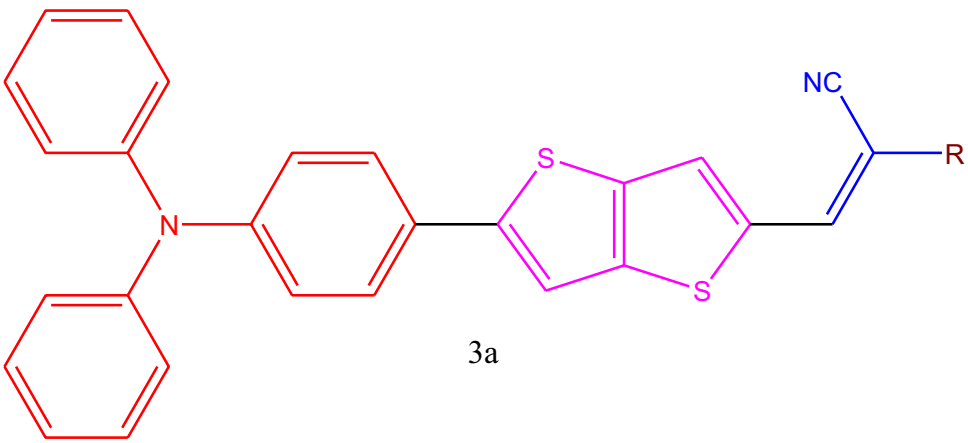

3a

R- CSSH, CONHOH, OH, PO3H2, SO2H

that the $\eta_{collect}$ is a constant. As a consequence, the enhancement of the J_{SC} most attention on the LHE (λ) and Φ_{inject}.

LHE (λ) can be described by following Eq. (3) [37]:

$$LHE = 1 - 10^{-f} \tag{3}$$

where f is the oscillator strength of associated dye molecules concerning the λ_{max}. To achieve a large f value, the dye sensitizers must have greater light absorption abilities in a wide spectrum of sunlight to certify a well light capture.

ΔG_{inject} can be illustrated by following Eq. (4) [38]:

$$\Delta G_{inject} = E_{OX}^{dye^*} - E_{CB}^{TiO_2} \tag{4}$$

Here, $E_{OX}^{dye^*}$ the reduction potential of the energy excited state dyes and $E_{CB}^{TiO_2}$ conduction band of TiO_2. Here, CBE of TiO_2 surface (-4.0 eV) has been used in this work, which is extensively used in theoretical research of DSSCs. $E_{OX}^{dye^*}$ can be expressed as following Eq. (5) [39]:

$$E_{OX}^{dye^*} = E_{OX}^{dye} - \lambda_{max}^{ICT} \tag{5}$$

Here, E_{OX}^{dye} the ground state of dyes in the oxidation potential energy, while λ_{max}^{ICT} is the maximum energy of ICT. Regeneration efficiency of dye η_{reg} is also a consequence by the J_{SC}, which is determined by the driving force of regeneration ΔG_{reg}, it can be communicated as follows [40]:

$$\Delta G_{reg} = E_{redox} - E_{OX}^{dye} \tag{6}$$

In this study, the redox potential of the liquid electrolyte (−4.8 eV) has been used. As for V_{OC} in DSSCs, it can be described by following Eq. (7) [41]:

$$V_{OC} = \frac{E_{CB} + \Delta CB}{q} + \frac{KT}{q} \ln\left[\frac{n_C}{N_{CB}}\right] - \frac{E_{redox}}{q} \tag{7}$$

The energy difference between the semiconductor CBE and redox electrolyte is also calculated by Eq. (7). E_{redox} signifies redox potential of the Fermi level. Usually, the I^-/I_3^- electrolyte solution has a constant redox potential value. ΔCBE is the significant factor V_{OC}, it can be described as follows [42]:

$$\Delta CBE = -\frac{q\mu_{normal}\gamma}{\varepsilon_0\varepsilon} \tag{8}$$

From Eq. (8), q is the elementary charge, γ is the molecular outermost level surface concentration, μ_{normal} denotes the vertical dipole moment of the absorbed dye to the CBE of TiO_2 substrate, ε_0, ε as the vacuum and dielectric permittivity, respectively. If the dipole moment value higher also higher the open-circuit photovoltage. The maximum theoretical values of the eV_{OC} between the E_{LUMO} and E_{CB}, it can be stated by the following Eq. (9) [43]:

$$eV_{OC} = E_{LUMO} - E_{CB} \tag{9}$$

Computational details

The ground-state molecular geometries of all A1–A5 molecules were fully optimized by the B3LYP [44] functional and 6-31G(d) basis set of all atoms. The optimized structures are implemented without any symmetry constraints, which is commonly used for computational research. Also, optimized dyes were confirmed to be at its local minima (no imaginary frequency modes) on the potential energy surfaces.

The electronic distribution of the molecular orbitals has been calculated to display the position of the electron localization. The preceding evaluation suggests that TD-DFT is extremely reliable inside the calculation of vertical excitation energy and PV properties [45, 46]. To select the reliability, it may use a hybrid exchange-correlation (XC) and long-range correlated (LC) functionals using for CT excitations show great consequences. Hence, there are numerous XC functionals were made to deliver a good description of molecules excited states absorption. To select suitable functionals, which assume XC and LC functionals, including B3LYP, CAM-B3LYP [47] and ωB97XD [48] has been calculated absorption wavelength in TD-DFT strategies. Thus, based on 3a geometry, the TD-DFT method with suitable functionals and 6-31G(d) basis set were executed to get the absorption peak and oscillator strength of dyes. From these functionals, the optical absorption peak of 3a dyes was 163, 470 and 454 nm, respectively. The theoretical peak of selected functionals results and corresponding experimental data are shown in Fig. 1 and Table 1. From the figure and table, ωB97XD method was better matched to the literature 455 nm with errors more or less than 68, 15 and 01 nm. As a result, the TD-ωB97XD/6-31G(d) technique is discovered to be the best reliable level for the prediction of absorption spectra. Therefore, the electronic UV–Vis spectra and vertical oscillator strengths of the A1–A5 dyes have been executed by TD-ωB97XD/6-31G(d) technique in this study. As per the literature, ethanol solvent effects have been included via the conductor-like polarizable continuum model (C-PCM) [34, 49, 50]. The A1–A5 dye absorption wavelengths have been calculated by the usage of GaussSum software version 3.0 [51]. All calculations of the isolated dyes have been accomplished by the Gaussian 09w program package [52].

Results and discussion

Substituent effect of A1–A5 dyes

The electron acceptor group is a key parameter with a D-π-A structure for the high performance of organic DSSCs. We selected in particular five functional categories, which might

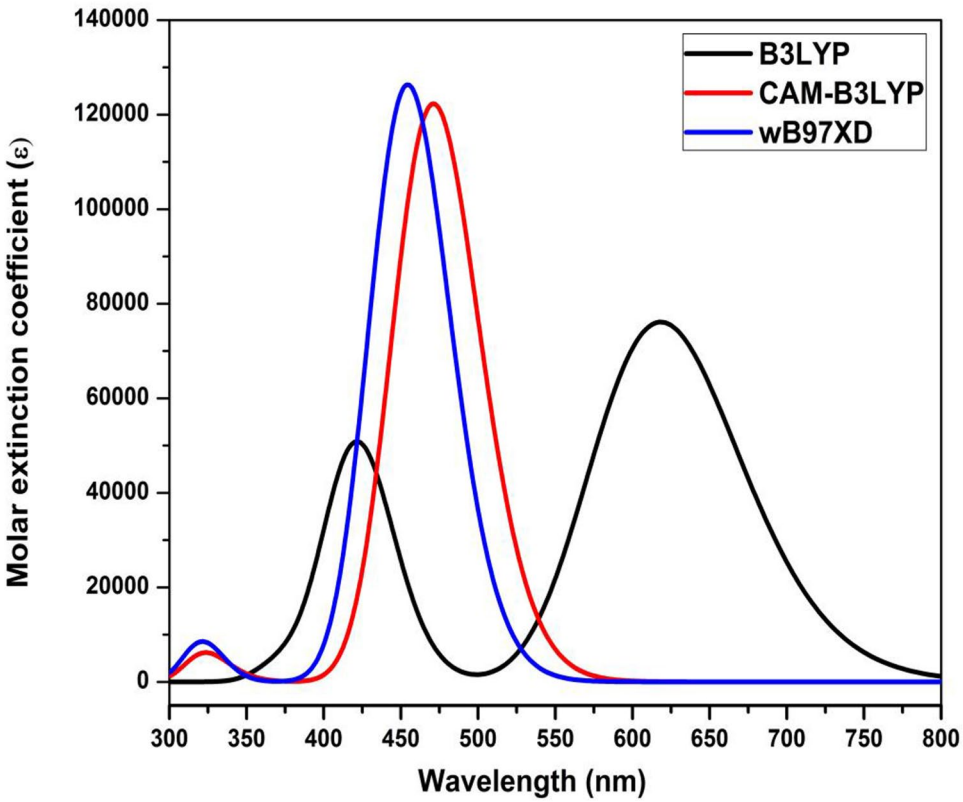

Fig. 1 TD-DFT absorption peak of 3a calculated at different functionals in THF solvent

Table 1 Experimental maximum absorption peak, computed vertical excitation energies of the lowest excited state λ_{max} (nm), oscillator strengths (*f*) and major orbital configurations of 3a dye is implemented on different functionals with ethanol solvent medium using TD-DFT method

Methods	λ_{max} (nm)	Oscillator strength (*f*)	Main configuration (%)
B3LYP	618	1.050	HOMO→LUMO (100%)
CAM-B3LYP	470	1.687	HOMO→LUMO (76%)
ωB97XD	454	1.743	HOMO→LUMO (65%)
Experiment	455	Taken from Ref. [33]	

be made for the addition of chemically altered in cyanoacrylic acid. Those are previously stated within the segment. The substituent acceptor unit has been given as collected from the literature. From the preceding look at, those altered groups are used in DSSCs application. In this work, these groups will be stimulated on the TPA-based dye derivatives. A series of newly designed dyes (A1–A5) based on 3a have been systematically investigated. The optimized geometric structures of the 3a and A1–A5 dyes have been implemented on the B3LYP/6-31G(d) theory and shown in Fig. 2. The geometric systems found out that the acceptor effect of A1–A5 has better coplanar, which benefits the electron CT from the D to A and accelerates electron injection to the CBE of TiO_2 surface. Furthermore, the effect of A1–A5 is vital for highly enhanced ICT character, which favors for the red-shift absorption spectra and PV parameters.

Frontier molecular orbitals energy levels (FMOs)

Frontier molecular orbitals (FMOs) of the organic dye molecules A1–A5 have been recognized concerning electron CT upon photoexcitation. The FMOs is a very crucial factor in defining the charge-separated states of dye sensitizers [53]. The impact of the electron acceptor in HOMOs and LUMOs has been studied. Figure 3 shows the isodensity contour plots of the CT for 3a and A1–A5 dyes. The electron dispersal of highest occupied molecular orbitals (HOMOs) is predominantly contained in the electron-D of TPA and π-spacer, while the electron spreading of lowest unoccupied molecular orbitals (LUMOs) is typically contained at the π-spacer and electron-A segment of cyanoacetic acid (generally on the anchoring area). This specifies that the good charge-divided state between HOMOs and LUMOs. Furthermore,

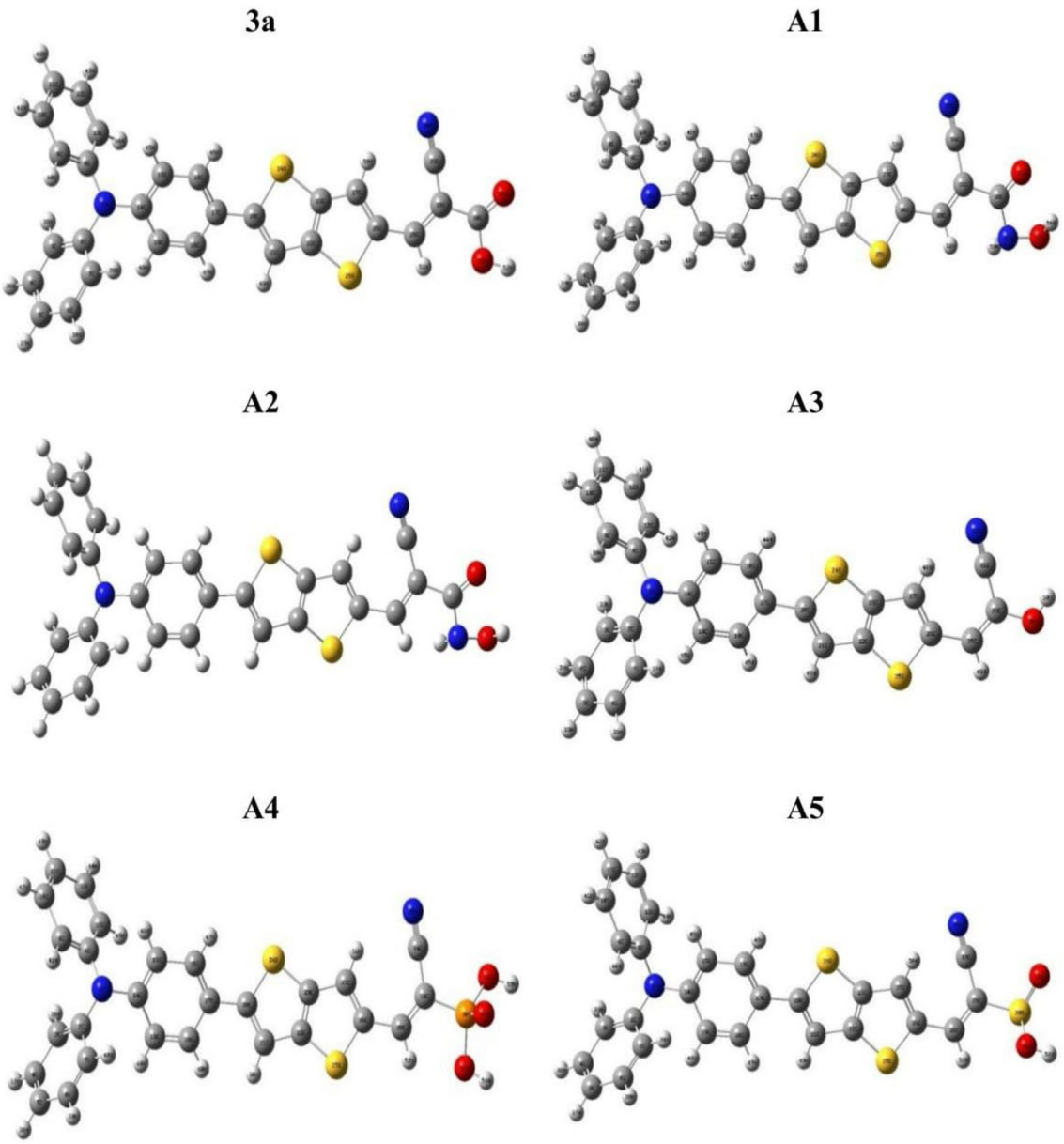

Fig. 2 Optimized geometric structures of 3a and designed dye molecules were calculated at B3LYP/6-31G(d) level of theory

the HOMOs and LUMOs of the dyes are a good separated CT process. The HOMOs energies of A1–A5 dyes are a possible response to the regeneration of the redox shuttle. The calculated results demonstrate that the HOMOs energies of dyes are lower than the redox I^-/I_3^- electrolyte. Similarly, LUMOs energy levels of A1–A5 dyes are higher than that of semiconductor CBE [54]. Consequently, LUMOs energies of all dyes are positive responses to injecting electrons into the CBE of TiO_2.

As shown in Fig. 4, all LUMOs are above the CBE of TiO_2 and the HOMOs are situated below the redox I^-/I_3^- electrolyte. According to Table 2, A1–A5 in dyes HOMOs and LUMOs values are − 5.25, − 5.20, − 5.49, − 5.09, − 5.03 eV and − 2.90, − 2.95, − 3.07, − 2.87, − 2.85 eV, respectively. The calculated energy gap (E_g) of the A1–A5 dye molecules, with the decreasing order of A3 > A1 > A2 > A4 > A5. The HOMOs and LOMOs energy levels show positively respond to the development of PV properties in organic DSSCs. As shown in Fig. 4, the energy level diagram of the A1–A5 dye sensitizers has a smaller energy gap of A5 in comparison with the other molecules and 3a dye. Therefore, it may be stated that the A1–A5 dyes take a positive response to the CT and regeneration related to the photo-oxidation process.

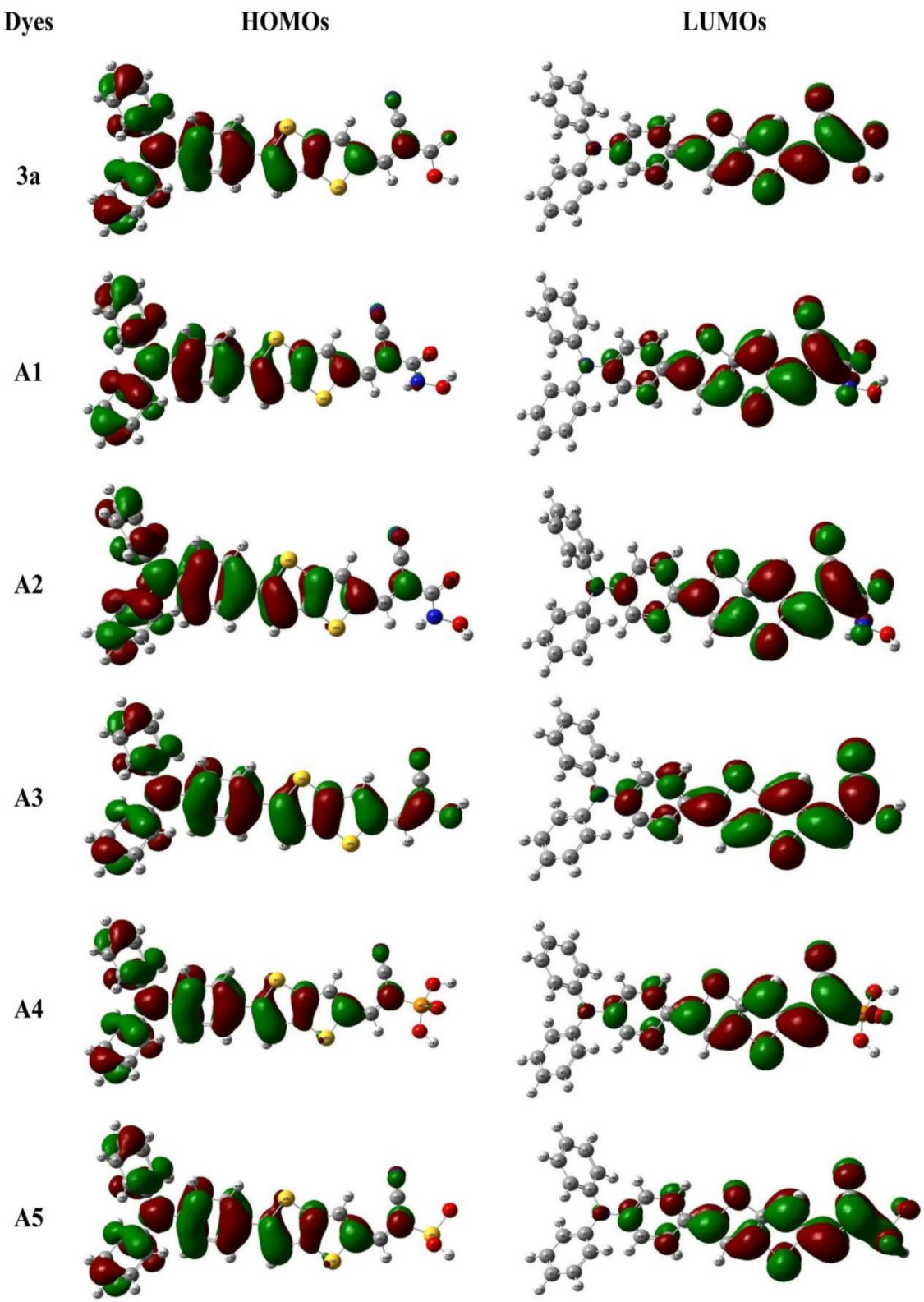

Fig. 3 The selected frontier molecular orbitals of the designed dye molecules and 3a dye were calculated at B3LYP/6-31G(d) level of theory

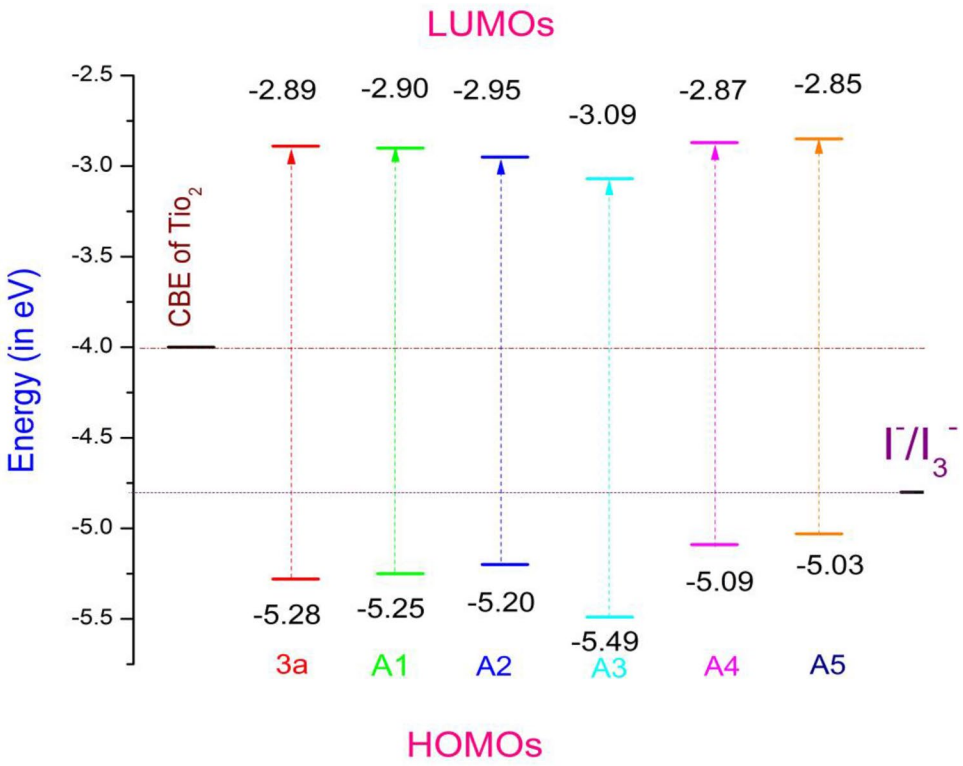

Fig. 4 The energy levels of the 3a and A1–A5 dyes were calculated by using B3LYP/6-31G(d) level of theory

Table 2 Molecular orbitals energy level of HOMOs, LUMOs, corresponding energy gap of the 3a and A1–A5 dye molecules were performed by using B3LYP/6-31G(d) basis set

Dyes	HOMOs (in eV)	LUMOs	Energy gap
3a	− 5.28	− 2.89	2.39
A1	− 5.25	− 2.90	2.35
A2	− 5.20	− 2.95	2.25
A3	− 5.49	− 3.07	2.42
A4	− 5.09	− 2.87	2.22
A5	− 5.03	− 2.85	2.18

Electronic absorption properties

The electronic absorption spectra of the 3a and A1–A5 dye molecules have been calculated by using TD-ωB97XD/6-31G(d) level of theory in an ethanol solvent medium. The calculated values of the A1–A5 molecules in vertical excitation energies (*E*), oscillator strengths (*f*), *LHE* and major orbital contributions were summarized in Table 3. Also, the corresponding simulated absorption spectra of the 3a and A1–A5 dyes have been shown in Fig. 5. All A1–A5 organic dyes are extensive visible around 600 nm, it is related to ICT property. Normally, the molecular dyes with broad absorption spectra and higher molar extinction coefficients are predicted to enhanced photo-to-current conversion efficiency performance [55]. The maximum absorption peaks of A5, A4, A2, A1 and A3 were 465, 456, 451, 448 and

Table 3 Optical absorption wavelengths corresponding excitation energies (λ_{max} in nm and eV), oscillator strength (f in a.u.), major orbital transitions (%) and light-harvesting efficiency (*LHE*) of the 3a, A1–A5 dyes are implemented by the TD-ωB97XD/6-31G(d) basis set in ethanol medium

Dyes	Wavelength		Oscillator strength (*f*)	LHE	Major transitions (%)
	Energy (eV)	λ_{max} (nm)			
3a	2.73	454	1.743	0.981	HOMO → LUMO (65%)
A1	2.76	448	1.742	0.981	HOMO → LUMO (65%)
A2	2.74	451	1.751	0.982	HOMO → LUMO (68%)
A3	3.02	409	1.605	0.975	HOMO → LUMO (71%)
A4	2.71	456	1.767	0.982	HOMO → LUMO (69%)
A5	2.66	465	1.807	0.984	HOMO → LUMO (69%)

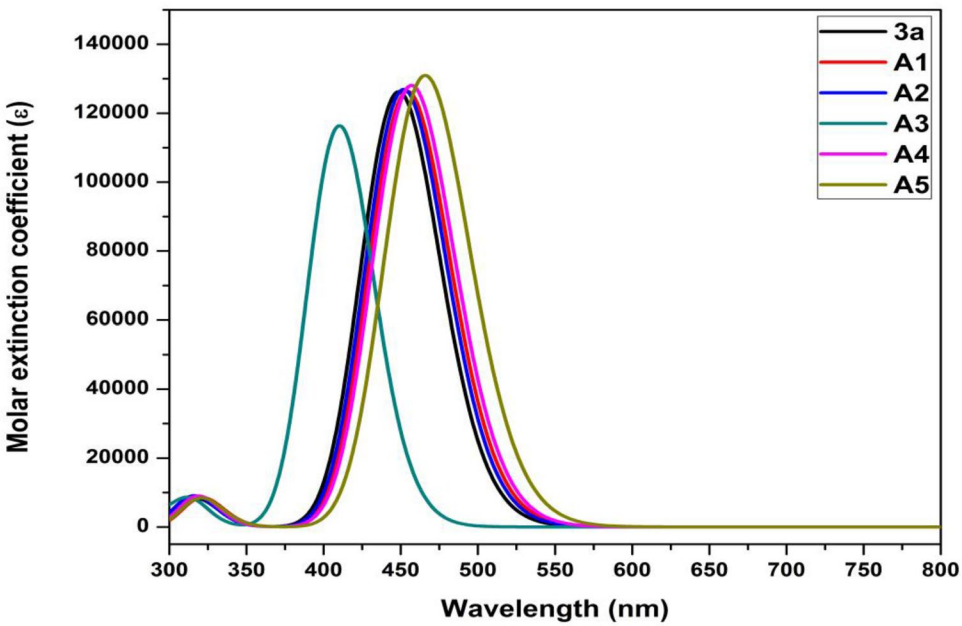

Fig. 5 TD-DFT absorption spectra of A1–A5 and 3a dyes were calculated by using ωB97XD/6-31G(d) level of theory in ethanol medium

409 nm, respectively. Wherein, A4, A5 have shown redshifts and A2, A1, A3 dyes showed blue-shifts compared to 3a (454 nm). The elongated absorption peak has been assigned to the ICT among the electron-D to electron-A and the shorter absorption spectra are assigned to the localized π-π* transitions within organic dye molecules. The dominant absorption spectra of A5 dye is observed at 465 nm compared to other molecules and 3a dye. In Table 3, vertical excitation energies (E) were changed in decreasing order of A3 > A1 > A2 > A4 > A5, showing that there is a redshift when passing from A3 to A5. Also, the first absorption peak belongs to the n–π* transition. The calculated results signify that the A4 and A5 dye molecules to display more on the long-wavelength side, which was promoting the higher performance of the corresponding DSSCs.

Overall efficiency

LHE and ΔG_{inject} are the two main influencing factors on J_{SC}, it also discussed above Eq. (2). The *LHE* is a vital factor for the organic dyes in considering the part of DSSCs, i.e., absorbing photons and injecting photoexcited electrons to the CBE of TiO_2 [56]. To give an impression about how the acceptor groups affect the *LHE*, we stimulated the UV–VIS absorption spectra of the dyes. The substituent effect of acceptor oscillator strengths is slightly changed in the entire visible region. *LHE* values of the organic dyes are given in a range (1.605–1.807) summarized in Table 4. Based on the literature, the *LHE* values have to be as high as possible to maximize the photocurrent response for DSSCs. Accordingly, A1–A5 dye sensitizers provide more or less similar photocurrent. Particularly, A4 and A5 dyes are maximizing the photocurrent response to the corresponding DSSCs, compared with 3a. Any other manner of improving J_{SC} is

Table 4 The calculated redox potential of the ground state (E^{dye} in eV), oxidation potential (E^{dye^*} in eV), vertical excitation energy (λ_{max} in eV), electron injection (ΔG_{inject} in eV), dye regeneration (ΔG_{reg} in eV) and open-circuit photovoltage (eV_{OC}) of the studied dye molecules are implemented on the TD-ωB97XD/6-31G(d) basis set in ethanol solvent medium

Dyes	E^{dye} in (eV)	λ_{max}	E^{dye^*}	ΔG_{inject}	ΔG_{reg}	eV_{OC}	Dipole moment (Debye)
3a	5.28	2.73	2.55	−1.45	0.48	1.11	10.42
A1	5.25	2.76	2.49	−1.51	0.45	1.10	11.38
A2	5.20	2.74	2.46	−1.54	0.40	1.05	13.06
A3	5.49	3.02	2.47	−1.53	0.69	0.93	4.28
A4	5.09	2.71	2.38	−1.62	0.29	1.13	15.59
A5	5.03	2.66	2.37	−1.63	0.23	1.15	16.50

to increase the electron injection efficiency of free energy ΔG_{inject}. As noted above, the calculation details for the determination of ΔG_{inject} and $E_{OX}^{dye^*}$ have been described in Eqs. (4 and 5). Based on Eqs. (4 and 5), A1–A5 dyes ΔG_{inject} and $E_{OX}^{dye^*}$ calculated values have been shown in Table 4. From the table, ΔG_{inject} absolute values are − 1.51, − 1.54, − 1.53, − 1.51, − 1.62 and − 1.56 eV, respectively. According to Islam concept, $\Delta G_{inject} > 0.2$ eV [57]. Accordingly, A1–A5 dye molecules are greater than the 0.2 eV. As shown in Table 4; we find that these dyes have negative values ΔG_{inject}.

Besides, ΔG_{reg} might also affect the J_{SC} DSSCs, it can be calculated based on above Eq. (6). Accordingly, it is understandable that the larger μ_{normal}, the higher V_{OC}. From Table 4, the calculated values of A1–A5 dyes are 0.45, 0.40, 0.69, 0.29 and 0.23 eV, respectively. Particularly, A4 and A5 dye sensitizers can be the fastest regeneration compared to other dyes and 3a, which benefits increase J_{SC}. If μ_{normal} the value was high also higher V_{OC}. μ_{normal} is calculated based on above Eq. (8). From Table 4, dipole moment values of A1–A5 dyes are 11.38, 13.06, 4.28, 15.59 and 16.50 Debye, respectively. In particular, A4 and A5 dyes are the highest dipole moment, compared to other sensitizers and 3a (10.42 Debye), which benefits to larger V_{OC}.

It can be seen that a larger E_{LUMO} will produce a higher eV_{OC}. As displayed in Table 4, the eV_{OC} values of the A1–A5 dyes are 1.10, 1.05, 0.93, 1.13 and 1.15 eV, respectively. Here, A4 and A5 dyes have larger eV_{OC}, compared to other dyes and 3a (1.11 eV). Taking the μ_{normal} and eV_{OC} values into account, A4 and A5 dyes must have a larger V_{OC}. Accordingly, the results specify that the substituting effect of A4 and A5 dyes can enhance V_{OC}, which indicated outstanding performance. Finally, A4 and A5 may be the overall performance for excessive conversion efficiency of DSSCs.

Conclusion

A sequence of five isolated metal-free organic A1–A5 dyes based on electron acceptor have successfully studied the DSSCs application. The effect of the A1–A5 acceptor groups on the molecular orbital electronic structures, absorption properties, light-harvesting efficiency and photovoltaic performance of dyes have been systematically investigated. Furthermore, DFT and TD-DFT methods have been discussed in detail. The calculated outcomes suggest that the screened with an electron acceptor in A4 and A5 are promising functional organizations for the D-π-A structure. Moreover, the calculated results imply that the A4 and A5 dyes are strongly electron injection, charge transition, dye regeneration and increasing the dipole moment, which is the highest power conversion efficiency of DSSCs. Finally, our investigated results display that the dye molecules A1–A5, particularly A4 and A5 are promising applicants for high-efficiency organic DSSCs. It is concluded that the choice of the appropriate screen with an electron acceptor is very important for the molecular design of TPA dyes with highly efficient organic solar cells.

Acknowledgements The authors extend their sincere appreciation to the Researchers Supporting Project at King Saud University for funding this Research RSP-2020/29.

Compliance with ethical standards

Conflict of interest The authors declared that there is no conflict of interest.

References

1. B. O'Regan, M. Grätzel, Nature **353**, 737 (1991)
2. E.C. Prima, B. Yuliarto, V. Suendo, Suyatman, J. Mater. Sci.: Mater. Electron. **25**, 4603 (2014)
3. M.A. Green, K. Emery, Y. Hishikawa, W. Warta, Prog. Photovolt. Res. Appl. **18**, 346 (2010)
4. A. Mishra, M.K.R. Fischer, P. Bauerle, Angew. Chem. Int. Ed. **48**, 2474 (2009)
5. A. Hagfeldt, G. Boschloo, L.C. Sun, L. Kloo, H. Pettersson, Chem. Rev. **110**, 6595 (2010)
6. Y.S. Yen, H.H. Chou, Y.C. Chen, C.Y. Hsu, J.T. Lin, J. Mater. Chem. **22**, 8734 (2012)
7. Y.Z. Wu, W.H. Zhu, Chem. Soc. Rev. **42**, 2039 (2013)
8. A. Arunkumar, M. Prakasam, P.M. Anbarasan, Bull. Mater. Sci. **40**, 1389 (2017)
9. T. Kitamura, M. Ikeda, K. Shigaki, T. Inoue, N.A. Anderson, X. Ai, T. Lian, S. Yanagida, Chem. Mater. **16**, 1806 (2004)
10. K. Sayama, K. Hara, N. Mori, M. Satsuki, S. Suga, S. Tsukagoshi, Y. Abe, H. Sugihara, H. Arakawa, Chem. Commun. **13**, 1173 (2000)
11. A. Ehret, L. Stuhl, T.M. Spitler, J. Phys. Chem. B **105**, 9960 (2001)
12. Z. Wang, F.Y. Li, C.H. Huang, Chem. Commun. **20**, 2063 (2000)
13. M. Liang, W. Xu, F. Cai, P. Chen, B. Peng, J. Chen, Z. Li, J. Phys. Chem. C **111**, 4465 (2007)
14. M. Velusamy, K.R.J. Thomas, J.T. Lin, Y.C. Hsu, K.C. Ho, Org. Lett. **7**, 1899 (2005)
15. M.S. Tsai, Y.C. Hsu, J.T. Lin, H.C. Chen, C.P. Hsu, J. Phys. Chem. C **111**, 18785 (2007)
16. K.R.J. Thomas, Y.-C. Hsu, J.T. Lin, K.M. Lee, K.C. Ho, H.C. Lai, Y.-M. Cheng, P.-T. Chou, Chem. Mater. **20**, 1830 (2008)
17. K. Hara, T. Sato, R. Katoh, A. Furube, T. Yoshihara, M. Murai, M. Kurashige, S. Ito, A. Shinpo, S. Suga, H. Arakawa, Adv. Funct. Mater. **15**, 246 (2005)
18. A. Arunkumar, S. Shanavas, P.M. Anbarasan, J. Comput. Electron. **17**, 1410 (2018)
19. R. Chen, X. Yang, H. Tian, L. Sun, J. Photochem. Photobiol. A Chem. **189**, 295 (2007)
20. Z.S. Wang, K. Hara, Y. Dan-oh, C. Kasada, A. Shinpo, S. Suga, H. Arakawa, H. Sugihara, J. Phys. Chem. B **109**, 3907 (2005)
21. K. Hara, T. Sato, R. Katoh, A. Furube, Y. Ohga, A. Shinpo, S. Suga, K. Sayama, H. Sugihara, H. Arakawa, J. Phys. Chem. B **107**, 597 (2003)
22. K. Hara, M. Kurashige, D. Yasufumi, C. Kasada, A. Shinpo, S. Suga, K. Sayama, H. Arakawa, New J. Chem. **27**, 783 (2003)
23. H. Hara, K. Sayama, Y. Ohga, A. Shinpo, S. Suga, H.A. Arakawa, Chem. Commun. **6**, 569 (2001)

24. S. Ito, S.M. Zakeeruddin, R. Humphry-Baker, P. Liska, R. Charvet, P. Comte, M.K. Nazeeruddin, Adv. Mater. **18**, 1202 (2006)
25. L. Schmidt-Mende, U. Bach, R. Humphry-Baker, T. Horiuchi, H. Miura, S. Ito, S. Uchida, M. Grätzel, Adv. Mater. **17**, 813 (2005)
26. T. Horiuchi, H. Miura, S. Uchida, J. Photochem. Photobiol. A Chem. **164**, 29 (2004)
27. T. Horiuchi, H. Miura, K. Sumioka, S. Uchida, J. Am. Chem. Soc. **126**, 12218 (2004)
28. D. Kim, J.K. Lee, O. Kang, J. Ko, Tetrahedron **63**, 1913 (2007)
29. S. Kar, J.K. Roy, J. Leszczynski, NPJ Comput. Mater. **3**, 22 (2017)
30. S. Kim, J.K. Lee, S.O. Kang, J. Ko, J.H. Yum, S. Fantacci, F. De Angelis, D. Di Censo, M.K. Nazeeruddin, M. Grätzel, J. Am. Chem. Soc. **128**, 16701 (2006)
31. P. Liu, J.-J. Fu, M.-S. Guo, X. Zuo, Y. Liao, Comput. Theor. Chem. **1015**, 8 (2013)
32. J. Feng, Y. Jiao, W. Ma, M.K. Nazeeruddin, M. Grätzel, S. Meng, J. Phys. Chem. C **117**, 3772 (2013)
33. S.M. Fernandes, M.C.R. Castro, A.I. Pereira, A. Mendes, C. Serpa, J. Pina, L.L. Justino, H.D. Burrows, M.M.M. Raposo, ACS Omega **2**, 9268 (2017)
34. C. Zhao, X. Guo, J. Ma, H. Ge, L. Jin, Q. Zhang, Comput. Theor. Chem. **1105**, 89 (2017)
35. M.R. Narayan, Renew. Sustain. Energy Rev. **16**, 208 (2012)
36. J. Zhang, H.-B. Li, S.-L. Sun, Y. Geng, Y. Wu, Z.-M. Su, J. Mater. Chem. **22**, 568 (2012)
37. J. Preat, D. Jacquemin, C. Michaux, E.A. Perpète, Chem. Phys. **376**, 56 (2010)
38. R. Katoh, A. Furube, T. Yoshihara, K. Hara, G. Fujihashi, S. Takano, M. Tachiya, J. Phys. Chem. B **108**, 4818 (2004)
39. J. Zhang, Y.-H. Kan, H.-B. Li, Y. Geng, Y. Wu, Z.-M. Su, Dyes Pigments **95**, 313 (2012)
40. T. Daeneke, A.J. Mozer, Y. Uemura, S. Makuta, M. Fekete, Y. Tachibana, L. Spiccia, J. Am. Chem. Soc. **134**, 16925 (2012)
41. T. Marinado, K. Nonomura, J. Nissfolk, M.K. Karlsson, D.P. Hagberg, L. Sun, S. Mori, A. Hagfeldt, Langmuir **26**, 2592 (2009)
42. S. Rühle, M. Greenshtein, S.G. Chen, A. Merson, H. Pizem, C.S. Sukenik, D. Cahen, A. Zaban, J. Phys. Chem. B **109**, 18907 (2005)
43. W. Sang-aroon, S. Saekow, V. Amornkitbamrung, J. Photochem. Photobiol. A Chem. **35**, 236 (2012)
44. P.J. Stephens, F.J. Devlin, C.F.N. Chablowski, M. Frisch, J. Phys. Chem. **98**, 11623 (1994)
45. A. Arunkumar, P.M. Anbarasan, Struct. Chem. **29**, 967 (2018)
46. S. Meng, E. Kaxiras, M.K. Nazeeruddin, M. Gratzel, J. Phys. Chem. C **115**, 9276 (2011)
47. T. Yanai, D.P. Tew, N.C. Handy, Chem. Phys. Lett. **393**, 51 (2004)
48. Y.-S. Lin, G.-D. Li, S.-P. Mao, J.-D. Chai, J. Chem. Theory Comput. **9**, 263 (2012)
49. P. Ordon, A. Tachibana, J. Chem. Sci. **117**, 583 (2005)
50. A. Arunkumar, P.M. Anbarasan, J. Electron. Mater. **48**, 1522 (2019)
51. N.M. O'Boyle, A.L. Tenderholt, K.M. Langner, J. Comput. Chem. **29**, 839 (2008)
52. M.J. Frisch, G.W. Trucks, H.B. Schlegel, G.E. Scuseria, M.A. Robb, J.R. Cheeseman, G. Scalmani, V. Barone, B. Mennucci, G.A. Petersson, H. Nakatsuji, M. Caricato, X. Li, H.P. Hratchian, A.F. Izmaylov, J. Bloino, G. Zheng, J.L. Sonnenberg, M. Hada, M. Ehara, K. Toyota, R. Fukuda, J. Hasegawa, M. Ishida, T. Nakajima, Y. Honda, O. Kitao, H. Nakai, T. Vreven, J.A. Montgomery Jr., J.E. Peralta, F. Ogliaro, M.J. Bearpark, J. Heyd, E.N. Brothers, K.N. Kudin, V.N. Staroverov, R. Kobayashi, J. Normand, K. Raghavachari, A.P. Rendell, J.C. Burant, S.S. Iyengar, J. Tomasi, M. Cossi, N. Rega, N.J. Millam, M. Klene, J.E. Knox, J.B. Cross, V. Bakken, C. Adamo, J. Jaramillo, R. Gomperts, R.E. Stratmann, O. Yazyev, A.J. Austin, R. Cammi, C. Pomelli, J.W. Ochterski, R.L. Martin, K. Morokuma, V.G. Zakrzewski, G.A. Voth, P. Salvador, J.J. Dannenberg, S. Dapprich, A.D. Daniels, O. Farkas, J.B. Foresman, J.V. Ortiz, J. Cioslowski, D.J. Fox, *Gaussian 09* (Gaussian Inc., Wallingford, 2009)
53. S. Jungsuttiwong, R. Tarsang, T. Sudyoadsuk, V. Promarak, P. Khongpracha, S. Namuangruk, Org. Electron. **14**, 711 (2013)
54. J.B. Asbury, Y.Q. Wang, E. Hao, H.N. Ghosh, T. Lian, Res. Chem. Intermed. **27**, 393 (2001)
55. J. Gong, J. Liang, K. Sumathy, Renew. Sustain. Energy Rev. **16**, 5848 (2012)
56. A. Arunkumar, M. Deepana, S. Shanavas, R. Acevedo, P.M. Anbarasan, Chemistryselect **4**, 4097 (2019)
57. A. Islam, H. Sugihara, H. Arakawa, J. Photochem. Photobiol. A Chem. **158**, 131 (2003)